

Dynamical Entanglement and Cooperative Dynamics in Entangled Solutions of Ring and Linear Polymers

Davide Michieletto*

*School of Physics and Astronomy, University of Edinburgh,
Peter Guthrie Tait Road, Edinburgh, EH9 3FD, United Kingdom and
MRC Human Genetics Unit, Institute of Genetics and Molecular Medicine,
University of Edinburgh, North Crewe Rd, Edinburgh, EH4 2XU, United Kingdom*

Takahiro Sakaue†

*Department of Physics and Mathematics, Aoyama Gakuin University,
5-10-1 Fuchinobe, Chuo-ku, Sagami-hara, Japan and
PRESTO, Japan Science and Technology Agency (JST),
4-1-8 Honcho Kawaguchi, Saitama 332-0012, Japan*

Understanding how entanglements affect the behaviour of polymeric complex fluids is an open challenge in many fields. To elucidate the nature and consequence of entanglements in dense polymer solutions, we propose a novel method: a “dynamical entanglement analysis” (DEA) to extract spatio-temporal entanglement structures from the pair-wise displacement correlation of entangled chains. By applying this method to large-scale Molecular Dynamics simulations of linear and unknotted, nonconcatenated ring polymers, we find a strong and unexpected cooperative dynamics: the footprint of mutual *entrainment* between entangled chains. We show that DEA is a powerful and sensitive probe that reveals previously unnoticed, and architecture-dependent, spatio-temporal structures of dynamical entanglement in polymeric solutions. We also propose a mean-field approximation of our analysis which provides previously under-appreciated physical insights into the dynamics of generic entangled polymers. We envisage DEA will be useful to analyse the dynamical evolution of entanglements in generic polymeric systems such as blends and composites.

Entanglement is a fascinating and ubiquitous phenomenon in nature and yet a comprehensive microscopic theory of entanglement is still not established. While the tube and reptation models can approximate the material properties of entangled linear polymers [1, 2], there are systems for which these theories do not apply. Among the most notable there are dense solution of ring polymers [3–6]. Here, the global topological invariance of the system, i.e. the fact that unknotted and nonconcatenated ring polymers must remain so at all times, entails that the rings tend to collapse and to assume crumpled conformations which are not entangled with each other in a classical “tube-like” sense [6–12]. Since rings do not have ends to diffuse, the reptation theory and its more modern extensions – such as contour length fluctuations, constraint release or tube enlargement – cannot be applied [13–15]. In light of this, a way to define and formalise entanglement that is also valid for topologically non-trivial polymers, such as rings, blends [16] and higher order topological (or chimeric) polymers [17–21], is highly needed.

Here we propose to study the dynamical effect of topological constraints (TCs) by measuring the cooperative dynamics of entangled polymers in a complementary way with respect to other existing approaches, e.g. primitive path analysis [22–25] or constitutive equations [25, 26]. Importantly, while most of the existing methods focus on either static entanglement structures or self-correlations (such as self mean squared displacement or stress relaxation) here we utilize the information of the correlated motion of entangled polymers in order to obtain information on the

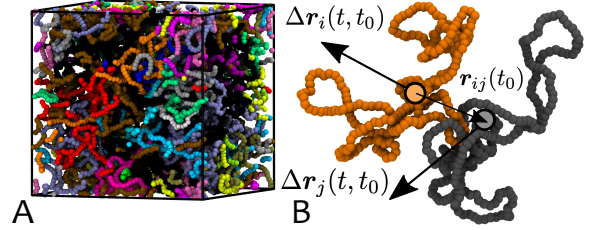


FIG. 1: **A** Snapshot from MD simulations of a dense solution of $M = 50$ ring polymers $N = 256$ beads long within a box of size $L = 50\sigma$ with periodic boundaries. **B** The dynamical entanglement analysis (DEA) proposed in this work probes the correlation between displacements $\Delta\mathbf{r}_i(t, t_0) = \mathbf{r}_i(t_0 + t) - \mathbf{r}_i(t_0)$ and $\Delta\mathbf{r}_j(t, t_0) = \mathbf{r}_j(t_0 + t) - \mathbf{r}_j(t_0)$ of two polymers i and j at lag-time t while recording their initial relative position $\mathbf{r}_{ij}(t_0) = \mathbf{r}_j(t_0) - \mathbf{r}_i(t_0)$. The correlation tensor $H(t, \mathbf{r})$ (Eq. (1)) encodes the propensity of two polymers at relative position \mathbf{r} to display correlated motion at timescale t .

space- and time-dependent entanglement structures. We dub this method *dynamical entanglement analysis* (DEA). [We also note that our approach to study cross-correlations (Fig. 1) is different from that of earlier works [27, 28]].

We apply DEA to large-scale Molecular Dynamics (MD) simulations of entangled systems of ring and linear polymers revealing qualitatively different spatio-temporal entanglement structures. Additionally, we link these numerical observations with phenomenological and mean-field theories which yield a renewed interpretation for the anomalous dynamics of entangled chains.

In practice, we consider M polymers N beads long in a cubic box of size L^3 with $\rho = M/L^3$ denoting

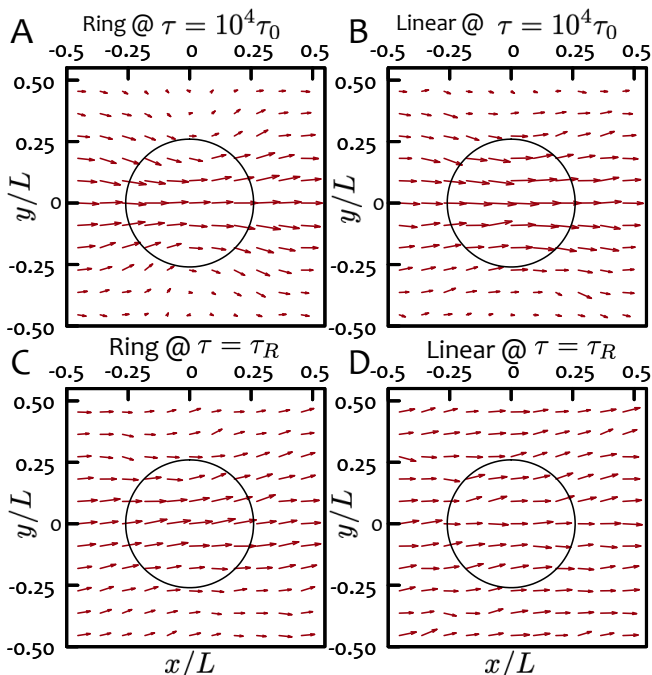


FIG. 2: 2D slice of the vector field $\mathbf{v}(t, \mathbf{r}) = H(t, \mathbf{r}) \cdot \mathbf{e}_x$ for ring and linear polymers $N = 512$ beads long at the lag-time (A-B) $t = 10^4 \tau_0$ and (C-D) $t = \tau_R = \tau_0 N^2 \simeq 26 \cdot 10^4 \tau_0$. Note that the vectors are scaled up or down for visualisation purposes: (A) $\times 2.5$ (B) $\times 20$ (C) $\times 0.125$ (D) $\times 1$. The circles are drawn using the average size R_g of the polymers as radii and note that the plots are normalised by the size of the box, which is different for ring and linear systems (see Table I in SI).

the concentration of chains and at monomer density $c = MN/L^3 = 0.1\sigma^{-3}$ (σ is the size of one bead). The polymers are semiflexible, i.e. have persistence length $l_p = 5\sigma$, chosen to lower the typical entanglement length (found to be $N_e = 40$ beads [29]) and to promote inter-ring threading [30]. A summarising table with the key parameters is given in the SI.

The correlation of displacement of different chains in the system can be computed as follows. Let $\mathbf{r}_i(t)$ be the position of centre of mass (CoM) of the i -th polymer at time t and $\Delta\mathbf{r}_i(t, t_0) = \mathbf{r}_i(t_0 + t) - \mathbf{r}_i(t_0)$ be its displacement during the lag time t . We define the displacement correlation tensor [31, 32] as

$$H_{\alpha\beta}(t, \mathbf{r}) \equiv \langle \Delta r_{i,\alpha}(t, t_0) \Delta r_{j,\beta}(t, t_0) \rangle_{\mathbf{r}}, \quad (1)$$

where the Greek indexes represent Cartesian components and the average $\langle \dots \rangle_{\mathbf{r}}$ is intended over times t_0 and pairs of polymers (i, j) , which satisfy $\mathbf{r}_{ij}(t_0) \equiv \mathbf{r}_j(t_0) - \mathbf{r}_i(t_0) = \mathbf{r}$ (see Fig. 1). We note that this formalism has been successfully employed in different contexts, e.g., in 2-point microrheology [32] and to investigate dynamics near the glass transition in colloidal systems [31] but has never been directly applied to systems of polymers. As we show below, Eq. (1) allows us to compute the correlation of the displacements at lagtime t between polymers at relative position \mathbf{r} (Fig. 1) and provides more spatiotemporal information on entanglements with respect to conventional self-correlations.

We compute $H(t, \mathbf{r})$ on our systems of polymers and

choose not to subtract the motion of the CoM of the whole system (see below and SI for details). To visualize the correlation tensor, we impose a fictitious, arbitrary displacement $\mathbf{e}_x = {}^t(1, 0, 0)$, and plot a 2D slice of the resulting 3D vector field $\mathbf{v}(t, \mathbf{r}) = H(t, \mathbf{r}) \cdot \mathbf{e}_x$ for fixed lag-times. In Fig. 2 we show two examples at $t = 10^4 \tau_0$ and $\tau_R \equiv \tau_0 N^2$, i.e. the Rouse time (we identify the microscopic time scale τ_0 with the Lennard-Jones (LJ) time $\tau_0 = \tau_{LJ} = \sigma\sqrt{m/\epsilon}$, where m is the mass and σ the size of a bead and $\epsilon = k_B T$ the energy scale of the LJ potential).

Figure 2 captures the most important conceptual finding of this paper, i.e. that we observe a highly coordinated pattern of the vector fields representing correlation of displacements. Importantly, such a persistent, coordinated pattern is not observed in unentangled and phantom chains (see Figs. S3 and S4 in SI). One should interpret these fields as the average displacement of a polymer at location \mathbf{r} from a probe polymer placed at the origin and that has displaced a unit length horizontally τ timesteps earlier. The strong alignment of the correlation vectors should not be confused with a flow of the polymers but is rather a signature of strong correlated dynamics and the consequence of entanglement among chains. We connect this correlation with the notion of “entrainment” – which amounts to a combination of steric and topological constraints between neighbouring polymers – that effectively results in the mutual “dragging” of neighbours and correlated motion that can persist at least up to the Rouse time, $\tau_R \sim N^2$. We note that the vectors in Fig. 2 are scaled up/down for visualisation purposes (see caption) and that the rings display much stronger cooperation with respect linear chains as their correlation vectors are typically longer (before rescaling). We stress that this is indication of rings being more entrained than linear chains of same length and that this is due to entanglement, as we observe no persistent coordinated correlation patterns in systems of phantom and unentangled polymers (see Figs. S3, S4 in SI). Furthermore, removing the overall CoM motion in this case effectively corresponds to constraining the overall flux of the correlation vector field over the simulation box to be almost zero (actually about $1/M$ as we show in the SI).

In order to further quantify this cooperative dynamics, we define the scalar quantity

$$\chi(t, \mathbf{r}) = \frac{\text{Tr}[H(t, \mathbf{r})]}{g_3(t)}, \quad (2)$$

which measures the degree of correlation during the time scale t between a pair of polymers that are initially separated by a distance $r = |\mathbf{r}|$. In Eq. (2), $g_3(t) = \langle (\mathbf{r}_{CM}(t_0+t) - \mathbf{r}_{CM}(t_0))^2 \rangle$ is the mean squared displacement (MSD) of the polymers’ CoM (or mean-squared self-displacement). [Note that $\text{Tr}[H(t, \mathbf{r})]$ is expected to depend only the separation $r = |\mathbf{r}|$ for homogeneous and isotropic system as the one considered here.] To elucidate the physical meaning of $\chi(t, \mathbf{r})$, imagine that we start to apply a force f in x direction at $t = 0$ only to the polymer i at the origin. This

force will cause an average displacement of polymer i that can be computed as $\langle \Delta r_{i,x}(t) \rangle = ft/\Gamma(t) = fg_3(t)/6k_B T$, where $\Gamma(t) = k_B T/D(t)$ is the effective friction, and $6D(t)t = g_3(t)$. At the same time, if chain i is entangled with chain j , it may cause the motion of chain j initially located at $\mathbf{r}_j(t_0) = \mathbf{r}$. Its average displacement can be calculated in a similar way as done for the probe chain:

$$\langle \Delta r_{j,\alpha}(t) \rangle_{\mathbf{r}} = \frac{H_{\alpha\beta}(t, \mathbf{r}) f_{\beta}}{2k_B T}, \quad (3)$$

where we generalise the mean-squared self-displacement in time (g_3) to include pair-wise correlation in space-time and along different directions via the time and space dependent tensor $H_{\alpha\beta}(t, \mathbf{r})$. For an isotropic system, we can take the angular average, leaving only the component along the direction of the force in Eq. (3), i.e. $\langle \Delta r_{j,x}(t) \rangle_{\mathbf{r}} = \frac{f}{6k_B T} \text{Tr}[H(t, \mathbf{r})]$. In the limit of perfect cooperativity $H_{\alpha\beta}(t, \mathbf{r}) = 2\delta_{\alpha\beta}D(t)t$ and the previous equation reduces to that for the probe chain.

In light of this, $\chi(t, r)$ can be seen as the ratio between the average displacement induced on polymer j and the average self-displacement of the probe i at time t and conditional to the fact that $|\mathbf{r}_i(t_0) - \mathbf{r}_j(t_0)| = r$. As such, $\chi(t, r)$ is bound to take values between 0 and 1, and may be thought as the fraction of monomers of polymer j that are effectively “dragged” – or entrained – by the motion of the (entangled) polymer i during the time scale t . Thus, the DEA naturally yields a quantity that has a physically appealing and intuitive meaning, that of how many monomers of polymer j at position r are entrained by i , t timesteps after that it has moved.

At long length- and time-scales, we expect the hydrodynamic behaviour with macroscopic viscosity η_b to dominate. In this regime $dH_{\alpha\beta}(t, \mathbf{r})/dt = (k_B T/8\pi\eta_b r)(\delta_{\alpha\beta} + \hat{r}_\alpha \hat{r}_\beta)$ is the Oseen tensor and $g_3(t) \simeq (k_B T/6\pi\eta_b R_g)t$. In this limit, $\chi(t, r)$ decays as $\sim R_g/r$. On the other hand, at length scales $r \lesssim R_g$, a cooperative motion will be predominantly caused by entanglements between polymers and $\chi(t, r)$ is thus expected to be a sensitive measure of the dynamically evolving entanglement.

In Fig. 3, we show $\chi(t, r)$ at different lag-times t and as function of r . One can notice that at short lag-times (Fig. 3A,B) $\chi(t, r)$ follows an architecture-dependent but length-independent master curve. In line with the magnitude of the vector field in Fig. 2, $\chi(t, r)$ also takes larger values for rings than for linear chains, with the latter catching up the former with time. The steep spatial gradient indicates that rings with overlapping CoMs (hence likely interpenetrating, or threading [30, 33–35]) are more correlated than distant ones. This spatial dependence is instead weaker for linear chains, indicating a more uniformly distributed entanglement structure over the whole contour of the chain, in qualitative agreement with the picture of the tube model. In other words, the structure of entanglements between neighbouring chains is qualitatively different between ring and linear chains,

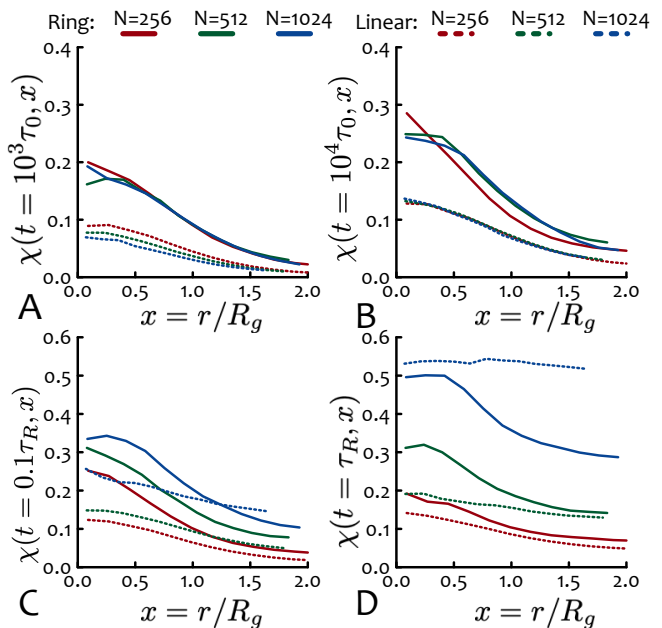


FIG. 3: Spatio-temporal evolution of dynamical cooperativity $\chi(t, r/R_g)$. This figure shows the spatial profile of $\chi(t, r)$ at fixed lag-times: (A) $t = 10^3 \tau_0$, (B) $t = 10^4 \tau_0$, (C) $t = 0.1\tau_R = 0.1\tau_0 N^2$ and (D) $t = \tau_R = \tau_0 N^2$. Notice that the lag-times in (C) and (D) are N dependent, hence the larger $\chi(t, r)$ values for longer chains. The maximum length-scale here is $L/2$ due to the periodic boundary conditions and is equivalent to $2R_g$ in our simulations.

and this difference is mirrored in weaker/stronger correlated motion shown in Fig. 2. We also stress that for phantom and unentangled chains, χ remains close to zero indicating that, as expected, there is no correlation at any spatial or temporal scales for non-entangled chains (see SI, Figs. S3 and S4).

To connect DEA with classic theories, we develop a mean-field approximation of our analysis in line with the mean-field approach of the tube theory. We calculate the spatial average of $\chi(t, r)$ as follows

$$\Xi(t) \equiv \frac{4\pi\rho \int_0^{r^*} r^2 g(r) \chi(t, r) dr}{4\pi\rho \int_0^{r^*} r^2 g(r) dr} \quad (4)$$

where $g(r)$ is the radial distribution function of the polymers’ centres of mass, and we take $r^* = L/2$ due to the periodic boundary condition. This quantity, plotted in Fig. 4, exhibits a power-law behavior in the short-medium time scale. The scaling of $\Xi(t)$ can be understood in light of the dynamical entanglement picture: since each chain has a number $P = 4\pi\rho \int_0^{r^*} r^2 g(r) dr$ of surrounding chains, i.e. those in the spherical volume of radius r^* , the number of monomers dragged by the motion of i -th ring is $\sim PN\Xi(t)$ and this provides an estimate for the effective friction experienced by each chain as $\Gamma(t) \simeq \gamma_0 PN\Xi(t)$ with γ_0 being a segment friction.

This effective friction on the global motion of the polymer can be compared with the theoretical predictions of the reptation theory for linear chains [2] and more recent theories for rings [37]. For linear polymers, the simplest reptation theory suggests [2] that $g_3(t) \sim \sigma^2(N_e^2/N)(t/\tau_e)^{1/2}$ for $\tau_e < t < \tau_R$,

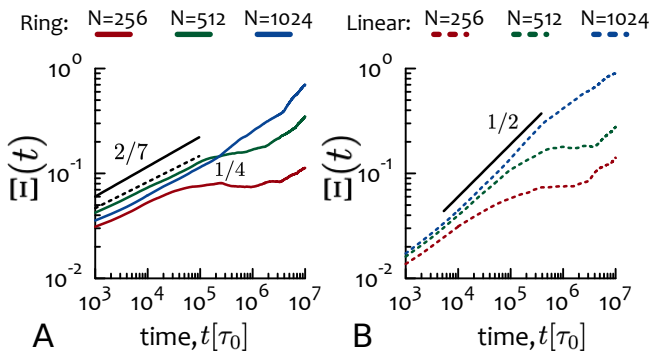


FIG. 4: Spatial average of the dynamical correlation, $\Xi(t)$, for (A) rings and (B) linear chains. The scaling for rings, $\sim t^{2/7}$ and $\sim t^{1/4}$ are obtained from Eq.(5) with $d_f = 3$ (crumpled globule) and $d_f = 5/2$ (Cates-Deutsch crossover [7, 36], see SI), respectively. For linear chains our calculation agrees with the classical reptation picture which predicts $\Xi(t) \sim t^{1/2}$ (see Eq.(5)).

where $N_e \simeq 40$ [6, 30] is the entanglement length and $\tau_e \sim \tau_0 N_e^2$ is the relaxation time for the entanglement lengthscale. For non-concatenated ring polymers, the conformation and the dynamics are self-similar [4, 6, 8, 37] for chain sections that are longer than N_e and on time scales $\tau_e < t < \tau_c$, where τ_c is the longest conformational relaxation time. According to the loopy-globule model [37], $\tau_c \sim \tau_e (N/N_e)^{(2d_f+1)/d_f}$, which may be thought as an analogue of the Rouse time in the linear chain counterpart (d_f denotes the fractal dimension of the ring conformation at the scale larger than the entanglement length). As shown in SI, the MSD of mass center turns out to be $g_3(t) \sim \sigma^2 (N_e^2/N) (t/\tau_e)^{(d_f+2)/(2d_f+1)}$ for $\tau_e < t < \tau_c$. With the help of the Einstein relation, these considerations lead to the effective friction $\Gamma(t) \simeq (k_B T/g_3(t))t$, which scales as

$$\Gamma(t) \sim \Xi(t) \sim \begin{cases} t^{1/2} & (\tau_e < t < \tau_R) \text{ linear} \\ t^{2/7} & (\tau_e < t < \tau_c) \text{ ring } d_f = 3 \end{cases} \quad (5)$$

in good agreement with the numerical observation in Fig. 4. Note the exponent for ring becomes 1/4 if we adopt the effective fractal dimension $d_f = 2.5$ which is more appropriate for rings with intermediate length [7, 36] (see also SI).

A further insight on the dynamical entanglement might be obtained by the following consideration for linear chains: there are $X_0 \equiv N/N_e$ polymers, on average, entangled with the i -th chain. In our picture, each entangled chain is entrained by the motion of the i -th chain, but such a response does not take place immediately but progressively and following the propagation of the tension from the entanglement points [38, 39]. For linear chains, the Rouse model predicts that $n(t) \sim N_e (t/\tau_e)^{1/2}$ monomers (counting from each entanglement point) move coherently with the i -th chain and thus contribute to the friction at time scale $\tau_e < t < \tau_R$. This leads to the effective friction

$$\Gamma_{\text{linear}}(t) \sim \gamma_0 N_e \left(\frac{n(t)}{N_e} \right) \times X_0 \quad (\tau_e < t < \tau_R). \quad (6)$$

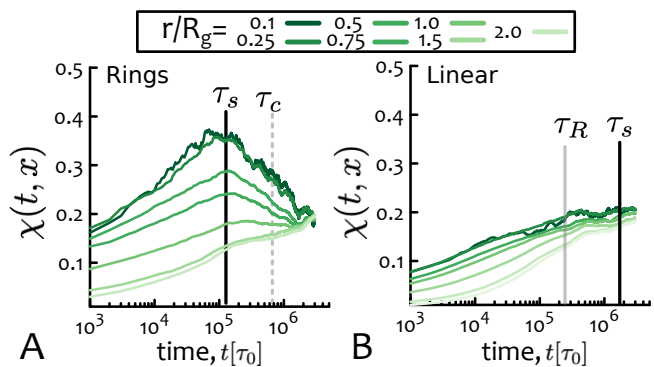


FIG. 5: Displacement correlations display a topology-dependent behaviour. We compare $\chi(t, r)$ (Eq. (2)) for (A) ring and (B) linear chains against time for increasing distances r/R_g and for fixed polymer length $N = 512$. In the figure, τ_s represents the self-diffusion time of the polymers, i.e. $g_3(\tau_s) \equiv R_g^2$ (see SI for $g_3(t)$ curves), $\tau_c = \tau_0 N_e^{-1/3} N^{7/3}$ the longest conformational relaxation time for rings and $\tau_R = \tau_0 N^2$ the Rouse time. Notice the non-monotonic behaviour of $\chi(t, r)$ at short length-scales that is peculiar for rings and indicating that the number of entanglements changes in time in systems of rings.

Besides being in agreement with Eq. (5), the above discussion provides a physically appealing picture for the well-established $g_3(t) \sim t^{1/2}$ scaling for the polymers' CoM motion in systems of linear chains. Now, anticipating a similar argument for ring polymers, we rewrite this effective friction as

$$\Gamma_{\text{ring}}(t) \sim \gamma_0 N_e \left(\frac{n(t)}{N_e} \right) \times X(t) \quad (\tau_e < t < \tau_c) \quad (7)$$

and require it to match Eq. (5), where $n(t)$ and $\Gamma_{\text{ring}}(t)$ are obtained from the loopy-globule model (see SI). Remarkably, we find that the number of entangled chains is now time-scale dependent and it takes the form

$$X(t) = X_0 \left(\frac{n(t)}{N_e} \right)^{-1/d_f} \sim X_0 \left(\frac{t}{\tau_e} \right)^{-1/(2d_f+1)}. \quad (8)$$

The number of entangled rings will thus be reduced from $X_0 = N/N_e$ at $t = \tau_e$ to $(N/N_e)^{1-(1/d_f)}$ at $t = \tau_c$. Such a feature is absent in the entangled linear polymers for which they have, on average, the same number of entangled chains at all times. Thus the predicted power-law scaling for the number of entangled chains represents a unique feature in ring polymers system, which is akin to a tube dilation effect proposed in the loopy globule model [37]. Note that in solutions in which N/N_e exceeds the coordination number (or the overlap parameter) $\sim R^3/N\sigma^3$, which scales as $\sim N^{1/2}$ for linear chains but takes constant value of about 15 – 20 for rings [6, 40], the above discussion may require some modification [41].

Discussion – Using DEA, we find that a chain mobility is dictated by entanglement-driven *entrainment*, and that the number of such entrained segments increases in time due to the propagation of entanglements up to the Rouse time τ_R for linear chains and the conformational relaxation time τ_c for rings. Beyond these time scales, our current data does not allow

a quantitative discussion because of the insufficient statistics, but it is certainly interesting to explore the behavior of displacement correlation in such a longer time scale or larger systems. As a preliminary discussion, we show in Fig. 5 the spatio-temporal evolution of $\chi(t, r)$, now plotting several curves at fixed length scale r and as a function of time. Several marked differences between ring and linear chains are evident but the most remarkable is the following: for linear chains, $\chi(t, r)$ increases until the self-diffusion time τ_s (defined as $g_3(\tau_s) = R_g^2$) suggesting that this coincides with the disentanglement time [1, 2, 38] at which the correlated motion by mutual entanglement/entrainment disappears. On the contrary, for ring polymers we see that $\chi(t, r)$ is non-monotonic and its decay at short length scales indicates – in agreement with our model discussed above – that the number of entangled rings $X(t)$ decreases in time (Eq. (8)). At the same time, the dynamical cooperativity at large length scales displays a monotonic increase even at times larger than the self-diffusion time, i.e. $t > \tau_s$, which can be understood as due to the remaining $X(\tau_s)$ entangled chain at τ_s yet to be released from the entrainment. Further, we observe remnants of increasing dynamical entanglement at τ_c and argue that these are fully consistent with, and indeed rationalise, previous results showing that the time to enter free diffusion is considerably longer than the self-diffusion and conformational relaxation times ($\sim \tau_c$) in the dense solution of rings [4, 30, 34, 42]. A possible scenario for such a slow diffusion phenomenology is to invoke a mandatory cooperative structural rearrangement of rings [43], which may be related to the residual entanglement $X(\tau_c)$. We also argue that in the case of artificially frozen polymers [30, 42] or partially active ones [44], the entanglements that induce the entrainment found via DEA here may be the ones that induce the topological glass state.

Conclusions – We have shown that the DEA (Eq. (1)) can provide rich information on the spatial and temporal evolution of architecture-specific entanglements in polymer solutions. The proposed approach can be applied to various systems, e.g., from solutions of active polymers to chromosomes in vivo. For instance, a direct experimental realization of DEA may be feasible using fluorescently labelled actin or DNA [45]; while at present most of the experimental observables focus on self-correlations, it may be interesting to look at cross-correlation of differently-tagged molecules.

Furthermore, and additionally to the motion of the CoMs, it would be possible to analyse the interchain dynamic correlation at the segment scale, or perhaps more interestingly over an entanglement length scale; this may provide additional insights for instance clarifying finite size effects on DEA, which has not been done here. We also note that the surprisingly long and spatially extended cooperativity observed using DEA and the notion of *entrainment*, may explain the discrepancies of experiments with theories for linear [46] and ring [3] polymers and their long subdiffu-

sive regime compared with their self-diffusion time.

Finally, we highlight that our DEA can be applied to any polymeric system and we envisage interesting outcomes on entangled blends [16], composites [47, 48] or chimeric [17] polymer systems.

Acknowledgements. This work was in part supported by JSPS KAKENHI (No. JP18H05529) from MEXT, Japan, and JST, PRESTO (JPMJPR16N5). DM is supported by the Leverhulme Trust through an Early Career Fellowship (ECF-2019-088). TS thanks T. Ooshida for fruitful discussion on displacement correlation analysis. The authors would like to acknowledge networking support by the COST Action CA17139.

* davide.michieletto@ed.ac.uk

† sakaue@phys.aoyama.ac.jp

- [1] P. G. de Gennes, *Scaling concepts in polymer physics* (Cornell University Press, 1979).
- [2] M. Doi and S. F. Edwards, *The theory of polymer dynamics*, vol. 73 (oxford university press, 1988).
- [3] M. Kapnistos, M. Lang, D. Vlassopoulos, W. Pyckhout-Hintzen, D. Richter, D. Cho, T. Chang, and M. Rubinstein, *Nature materials* **7**, 997 (2008).
- [4] J. D. Halverson, W. B. Lee, G. S. Grest, A. Y. Grosberg, and K. Kremer, *The Journal of chemical physics* **134**, 204905 (2011).
- [5] A. R. Brás, R. Pasquino, T. Koukoulas, G. Tsolou, O. Holderer, A. Radulescu, J. Allgaier, V. G. Mavrantzas, W. Pyckhout-Hintzen, A. Wischniewski, et al., *Soft Matter* **7**, 11169 (2011).
- [6] A. Rosa and R. Everaers, *Physical review letters* **112**, 118302 (2014).
- [7] M. Cates and J. Deutsch, *J. Phys.* **47**, 2121 (1986).
- [8] M. Rubinstein, *Phys. Rev. Lett.* **57**, 3023 (1986).
- [9] T. Sakaue, *Physical review letters* **106**, 167802 (2011).
- [10] M. Lang, J. Fischer, and J. U. Sommer, *Macromolecules* **45**, 7642 (2012).
- [11] S. Obukhov, A. Johner, J. Baschnagel, H. Meyer, and J. P. Wittmer, *EPL (Europhysics Lett.)* **105**, 48005 (2014).
- [12] T. Sakaue and C. H. Nakajima, *Physical Review E* **93**, 2502 (2016).
- [13] T. McLeish, *Nature materials* **7**, 933 (2008).
- [14] M. Doi, *Journal of Polymer Science: Polymer Physics Edition* **21**, 667 (1983).
- [15] G. Marrucci, *Journal of Polymer Science: Polymer Physics Edition* **23**, 159 (1985).
- [16] D. Parisi, J. Ahn, T. Chang, D. Vlassopoulos, and M. Rubinstein, *Macromolecules* **53**, 1685 (2020).
- [17] A. Rosa, J. Smrek, M. S. Turner, and D. Michieletto, *ACS Macro Letters* **0**, 743 (0).
- [18] Y. Doi, A. Takano, Y. Takahashi, and Y. Matsushita, *Macromolecules* **48**, 8667 (2015).
- [19] E. Uehara and T. Deguchi, *Journal of Chemical Physics* **145** (2016).
- [20] T. Deguchi and E. Uehara, *Polymers (Basel)*. **9**, 13 (2017).
- [21] F. Landuzzi, T. Nakamura, D. Michieletto, and T. Sakaue, *Physical Review Research* **033529**, 1 (2020).
- [22] R. Everaers, S. K. Sukumaran, G. S. Grest, C. Svaneborg, A. Sivasubramanian, and K. Kremer,

- Science (80-.). **303**, 823 (2004).
- [23] A. E. Likhtman, *Soft Matter* **10**, 1895 (2014).
- [24] A. E. Likhtman and M. Ponmurugan, *Macromolecules* **47**, 1470 (2014).
- [25] D. J. Read, K. Jagannathan, and A. E. Likhtman, *Macromolecules* **41**, 6843 (2008).
- [26] V. A. H. Boudara, D. J. Read, and J. Ramírez, *Journal of Rheology* **64**, 709 (2020).
- [27] H. W. Spiess, *Berichte der Bunsengesellschaft für physikalische Chemie* **91**, 1397 (1987).
- [28] J. Cao and A. E. Likhtman, *Physical Review Letters* **104**, 1 (2010).
- [29] A. Rosa and R. Everaers, *PLoS Comp. Biol.* **4**, 1 (2008).
- [30] D. Michieletto and M. S. Turner, *Proceedings of the National Academy of Sciences* **113**, 5195 (2016).
- [31] T. Ooshida, S. Goto, T. Matsumoto, and M. Otsuki, *Phys. Rev. E* **94**, 1 (2016).
- [32] J. C. Crocker, M. T. Valentine, E. R. Weeks, T. Gisler, P. D. Kaplan, A. G. Yodh, and D. A. Weitz, *Phys. Rev. Lett.* **85**, 888 (2000).
- [33] D. Michieletto, D. Marenduzzo, E. Orlandini, G. Alexander, and M. Turner, *ACS Macro Lett.* **3**, 255 (2014).
- [34] E. Lee, S. Kim, and Y. Jung, *Macromol. Rapid Commun.* **36**, 1115 (2015).
- [35] J. Smrek and A. Y. Grosberg, *ACS Macro Letters* **5**, 750 (2016).
- [36] J. D. Halverson, W. B. Lee, G. S. Grest, A. Y. Grosberg, and K. Kremer, *The Journal of chemical physics* **134**, 204904 (2011).
- [37] T. Ge, S. Panyukov, and M. Rubinstein, *Macromolecules* **49**, 708 (2016).
- [38] M. Rubinstein and H. R. Colby, *Polymer Physics* (Oxford University Press, 2003).
- [39] T. Sakaue, *Polymers* **8**, 1 (2016).
- [40] T. A. Kavassalis and J. Noolandi, *Phys. Rev. Lett.* **59**, 2674 (1987).
- [41] A. Ajdari, F. Brochard-Wyart, C. Gay, P. G. de Gennes, and J. L. Viovy, *Journal de Physique II* **5**, 491 (1995).
- [42] D. Michieletto, N. Nahali, and A. Rosa, *Phys. Rev. Lett.* **119**, 7801 (2017).
- [43] T. Sakaue, *Soft Matter* **14**, 7507 (2018).
- [44] J. Smrek, I. Chubak, C. N. Likos, and K. Kremer, *Nature Communications* **11**, 1 (2020).
- [45] M. Abadi, M. F. Serag, and S. Habuchi, *Nature Communications* **9** (2018).
- [46] C. M. Ylitalo, G. G. Fuller, J. A. Kornfield, and D. S. Pearson, *Macromolecules* **24**, 749 (1991).
- [47] D. Michieletto, R. Fitzpatrick, and R. M. Robertson-Anderson, *Soft Matter* pp. 6703–6717 (2019).
- [48] R. Fitzpatrick, D. Michieletto, K. R. Peddireddy, C. Hauer, C. Kyriillos, B. J. Gurmessa, and R. M. Robertson-anderson, *Phys. Rev. Lett.* **121**, 257801 (2018).